Available online at www.sciencedirect.com
SCIENCE DIRECT®
Journal of Sound and Vibration 262 (2003) 1223–1234
JOURNAL OF SOUND AND VIBRATION
www.elsevier.com/locate/jsvi

Letter to the Editor

Travelling-wave representations of diffraction using leaky-mode Green function expansions

S. Ivansson[a,*], J. Bishop[b]

[a] *Division of Systems Technology, Swedish Defence Research Agency, SE-172 90 Stockholm, Sweden*
[b] *Naval Undersea Warfare Center, Division Newport, Code 2123, Newport, RI 02841-1708, USA*

Received 6 June 2002; accepted 1 October 2002

1. Introduction

Classical ray theory allows physically attractive expansions of acoustic wave fields, and field components with a well-defined angle-time arrival structure can be isolated. As a result, semi-empirical scattering rules (such as Lambert's law in underwater acoustics) can be applied component-wise, and ray-based field representations often provide the most practical way of computing scattering and reverberation. Infinite amplitudes at a smooth caustic can be avoided by Airy-function corrections [1, Section 45.1; 2, Section 9-4] and diffraction rays [1, Section 54.4; 3], can be introduced to represent the field in a shadow zone. Even with such improvements, however, ray theory remains an approximation that is exact only at infinite frequency.

The travelling-wave expansion, obtained by a series expansion of a depth-dependent Green function [4], has been suggested as a way to extend the useful field decomposition of ray theory to finite frequencies in an exact way. Related hybrid ray-mode and ray-wavenumber-integration techniques and codes are widely used [5–8]. The travelling-wave expansion works well when the pertinent wavenumber integrals can be truncated to the propagating regime. As it stands, however, it turns out that the travelling-wave expansion fails in isolating grazing-ray diffraction beyond boundary-produced caustics as illustrated in Fig. 1. Here, the evanescent regime of wavenumbers is important [9]. As a consequence, for example, reverberation levels in shallow water with a downward-refracting sound-velocity profile will not be correctly modelled.

The aim of the present paper is to explain the mentioned failure and propose a suitable remedy. Revisiting the travelling-wave expansion in Section 2, it is shown that the pertinent wavenumber integrals do not in general converge at infinity because of exponential growth! To obtain convergent integrals with corresponding physically sound field components, it is necessary to recombine the integrand components. This is shown in Section 3. The recombinant travelling-wave expansions that are proposed can be used for exact modelling of single (with only one

*Corresponding author.
E-mail addresses: sveni@foi.se (S. Ivansson), bishopjl@npt.nuwc.navy.mil (J. Bishop).

0022-460X/03/$ - see front matter
doi:10.1016/S0022-460X(02)01430-X

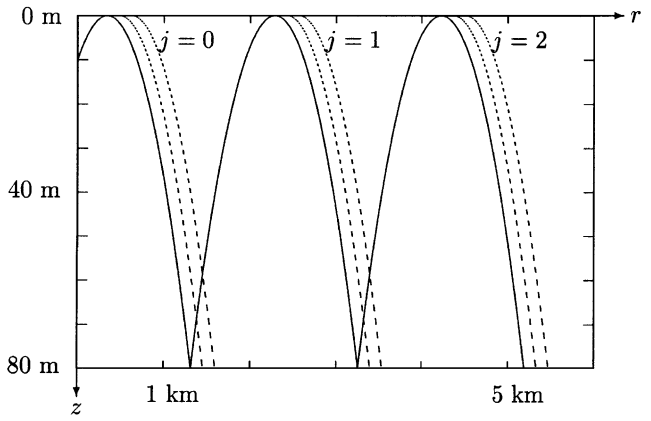

Fig. 1. The solid line in this r–z diagram is a grazing ray (the ray grazes the surface) that starts from a source at depth 10 m on the z-axis. Downward refraction is caused by a decrease of the sound speed $c(z)$ from 1.500 km/s at the surface (depth $z = 0$ m) to 1.480 km/s at the bottom ($z = 80$ m), in such a way that $1/c^2(z)$ is a linear function. The dashed lines for each j illustrate ray shedding, by horizontal displacements of the grazing ray at the surface, to produce single ($j = 0$) and multiple ($j = 1, 2, \ldots$) grazing-ray diffraction into the shadow zone for rays with j bottom bounces, that appears to the right of the corresponding downward going segment of the grazing ray. (The shadow will not be reached by a true ray, since a steeper one will be reflected at the surface and a less steep one will turn below the surface. For $j = 0$, this is well illustrated by Ref. [2, Fig. 9–17].)

interaction with the boundary, $j = 0$ in Fig. 1) as well as multiple ($j = 1, 2, \ldots$ in Fig. 1) grazing-ray diffraction.

For single grazing-ray diffraction, Brekhovskikh [1, Chapter IX] and Pierce [2, Section 9-5] have described how the shadow-zone field can be represented as a residues series, whose terms can be interpreted physically as ray shedding by diffraction rays or creeping waves. Applications to aeroacoustics and underwater acoustics can be found in Refs. [10,11], respectively. The results in Section 3 allow a generalization to multiple grazing-ray diffraction for general sound-speed profiles. Physically, ray contributions arise from wavenumbers of stationary phase while ray shedding in the shadow zones arises from leaky modes (Section 3.2).

2. Revisiting the travelling-wave expansion

Mono-frequency acoustic wave propagation is considered with time dependence $\mathrm{e}^{-\mathrm{i}\omega t}$, ω being angular frequency. Denoting horizontal slowness by p, and horizontal wavenumber by $k = \omega p$,

$$P(r, z) = \frac{1}{2} \int_{-\infty}^{\infty} G(z; p) \mathrm{H}_0^{(1)}(\omega p r) \omega^2 p \, \mathrm{d}p \tag{1}$$

synthetizes the pressure field at range r and depth z in a laterally homogeneous medium from its wavenumber components [12]. There are several methods for computing the Green function $G(z)$ directly [12]. The travelling-wave expansion is needed, however, to extract directional field components at finite frequencies. To obtain the expansion, the medium is artificially considered to be locally homogeneous at certain specification depths, cf., Refs. [13, Chapter 6; 14, Section 1]. Reflection coefficients $\gamma_A(p)$ and $\gamma_B(p)$ may then be introduced for up- and down-going plane

waves, respectively, and the Green function $G(z)$ in Eq. (1) can be written, see Section 2.1 for details,

$$G(z) = (1 - \gamma_A\gamma_B)^{-1} \sum_{i=1}^{4} G_{i,0}(z) = \sum_{i=1}^{4} \sum_{j=0}^{\infty} G_{i,j}(z), \tag{2}$$

where the $G_{i,j}(z) = (\gamma_A\gamma_B)^j G_{i,0}(z)$ are component Green functions.

A standing-wave (normal mode) expansion appears as the residue contributions from the p such that $\gamma_A\gamma_B = 1$ (e.g., Ref. [14]), whereas a travelling-wave expansion [4] appears by applying the geometric series for $(1 - \gamma_A\gamma_B)^{-1}$ as indicated. The index i is intended to separate upgoing and downgoing waves at source as well as receiver, whereas the index j is thought of as a cycle number. The implied decomposition of $P(r, z)$ becomes, with 'generalized ray' components $P_{i,j}$,

$$P(r, z) = \sum_{i=1}^{4} \sum_{j=0}^{\infty} P_{i,j}(r, z), \quad P_{i,j}(r, z) = \frac{1}{2} \int_{-\infty}^{\infty} G_{i,j}(z; p) \mathrm{H}_0^{(1)}(\omega p r) \omega^2 p \, \mathrm{d}p. \tag{3}$$

With accurate numerical integration, this is intended to extend to finite frequencies the field decomposition of classical ray theory (which reappears by applying WKBJ and stationary-phase approximations).

2.1. Technical definitions

The Green function G in Eq. (1) satisfies the depth-separated wave equation

$$\rho(z)[\rho^{-1}(z)G'(z)]' + \omega^2\xi^2(z)G(z) = f_S(z). \tag{4}$$

Here, $c(z)$ and $\rho(z)$ define the sound-speed and density profiles, $\xi(z) = [1/c^2(z) - p^2]^{1/2}$, while $f_S(z; p)$ is the source-strength function for a vertical source array on the depth axis. The Green function becomes uniquely defined by the boundary conditions at the surface and at the bottom (e.g., Ref. [15, Section 3.1.1]). Let $F_U(z)$ and $F_L(z)$ be non-trivial solutions of the homogeneous version of Eq. (4), with vanishing right-hand side, that fullfil the boundary condition at the surface and at the bottom, respectively. For convenience, restriction will be made to receiver depths z below all sources, implying that $G(z)$ is proportional to $F_L(z)$. The *uppermost* source depth is denoted z_s.

The reflection coefficients γ_A and γ_B are introduced in terms of two linearly independent solutions $F_-(z)$ and $F_+(z)$ of the homogeneous version of Eq. (4), where F_- and F_+ should be upgoing and downgoing in some sense, respectively. Specifically, $F_-(z) + \gamma_A F_+(z)$ is required to be proportional to $F_U(z)$, and $F_+(z) + \gamma_B F_-(z)$ is required to be proportional to $F_L(z)$. Hence, $W(F_- + \gamma_A F_+, F_U) = 0$ and $W(F_+ + \gamma_B F_-, F_L) = 0$, where the notation $W(H_1, H_2)$ is used for the depth-invariant Wronskian

$$W(H_1, H_2) = \rho^{-1}(H_1 H_2' - H_2 H_1') \tag{5}$$

involving two arbitrary solutions H_1 and H_2 of $\rho(z)[\rho^{-1}(z)H'(z)]' + \omega^2\xi^2(z)H(z) = 0$. It follows that

$$\gamma_A = -\frac{W(F_U, F_-)}{W(F_U, F_+)} \quad \text{and} \quad \gamma_B = -\frac{W(F_L, F_+)}{W(F_L, F_-)}. \tag{6}$$

To be able to proceed in terms of Wronskians, the source information contained in the function $f_S(z)$ needs to be reformulated. Let $\Phi_U(z)$ and $\Phi_L(z)$ be defined, for all z between the surface and the bottom, as the two unique solutions of Eq. (4) such that $\Phi_U(z) = 0$ for z above all sources while $\Phi_L(z) = 0$ for z below all sources. Apparently, $\rho(z)[\rho^{-1}(z)\Phi'(z)]' + \omega^2\xi^2(z)\Phi(z) = 0$ where $\Phi(z) = \Phi_U(z) - \Phi_L(z)$, and Wronskians involving Φ can be defined. Since receiver depths between the source depths will not be considered, the required source information is actually carried by the function Φ. To see this, note that there are numbers α and β such that $G(z) = \alpha[F_-(z) + \gamma_A F_+(z)] + \Phi_U(z) = \beta[F_+(z) + \gamma_B F_-(z)] + \Phi_L(z)$, and solve for α and β by forming Wronskian relations with F_- and F_+. For z below all sources, it follows that

$$G(z) = \frac{W(F_- + \gamma_A F_+, \Phi)}{(1 - \gamma_A\gamma_B)W(F_-, F_+)}[F_+(z) + \gamma_B F_-(z)], \tag{7}$$

and the Green function components according to Eq. (2), behind the field decomposition (3), become

$$G_{1,j}(z) = W^{-1}(F_-, F_+)W(F_-, \Phi)\gamma_A^j\ \gamma_B^j F_+(z), \tag{8}$$

$$G_{2,j}(z) = W^{-1}(F_-, F_+)W(F_+, \Phi)\gamma_A^{j+1}\gamma_B^j F_+(z), \tag{9}$$

$$G_{3,j}(z) = W^{-1}(F_-, F_+)W(F_-, \Phi)\gamma_A^j\gamma_B^{j+1} F_-(z), \tag{10}$$

$$G_{4,j}(z) = W^{-1}(F_-, F_+)W(F_+, \Phi)\ \gamma_A^{j+1}\gamma_B^{j+1} F_-(z). \tag{11}$$

The factors F_- and F_+ indicate directionality at the receiver (upwards, downwards). By reciprocity, the factors $W(F_-, \Phi)$ and $W(F_+, \Phi)$ can be expected to indicate directionality at the sources (downwards, upwards). Indeed, $W(F_-, \Phi)$ and $W(F_+, \Phi)$ will be linear combinations of F_-, F_-' and F_+, F_+', respectively, as evaluated at the source depths. To see this, consider the case with a single point source at depth z_s and evaluate the depth-invariant Wronskians at z_s+, noting that $\Phi(z_s+) = \Phi_U(z_s+)$, $\Phi'(z_s+) = \Phi_U'(z_s+)$ where Φ_U, Φ_U' have source-strength dependent step discontinuities at z_s. The general case follows by superposition.

2.2. Directional coupling and loss of unidirectionality

It is unfortunately not possible to subdivide a field in an inhomogeneous medium into directional components in a canonical way [16]. As a choice, directionality is assigned at particular specification depths [9]: z_- for F_- and z_+ for F_+. The natural restriction is made that $z_- \leqslant z_+$.

Considering the medium as locally homogeneous at z_-, a solution close to z_- of the homogeneous version of Eq. (4) will be a linear combination of $\exp(-\mathrm{i}\omega(z - z_-)\xi(z_-))$ and $\exp(+\mathrm{i}\omega(z - z_-)\xi(z_-))$. These governing exponentials prescribe that a locally upgoing F_- should be defined, for each p, according to $F_-(z_-) = 1$, $F_-'(z_-) = -\mathrm{i}\omega\xi(z_-)$. Likewise, an F_+ locally downgoing at z_+ should be defined by $F_+(z_+) = 1$, $F_+'(z_+) = +\mathrm{i}\omega\xi(z_+)$. However, the upgoing/downgoing character of F_-/F_+ will in general be corrupted away from z_-/z_+ by internal reflections, cf., [13, Sections 3.2,3.3,6.3]. As a result, directional coupling is anticipated, meaning that each $P_{i,j}$ will contain energy that should preferably have appeared in other components. Different choices of specification depths produce different distributions of internal reflections and different expansions (albeit with a common correct sum for the total field), and the field

decomposition is inherently non-unique. Upon restriction to sound-speed profiles with exactly one local minimum (which may be at the surface or at the bottom), one can formulate

Proposition 1. *To avoid trapped modes* [17], *which would generate directional coupling at long ranges*, z_- *and* z_+ *should both be located at the depth of minimum sound speed.*

Proof. Fig. 2 a illustrates a sound-speed profile with a well-defined local minimum denoted z_{min}. According to the definition of γ_A and γ_B in Eq. (6), residue or mode-type singularities appear in

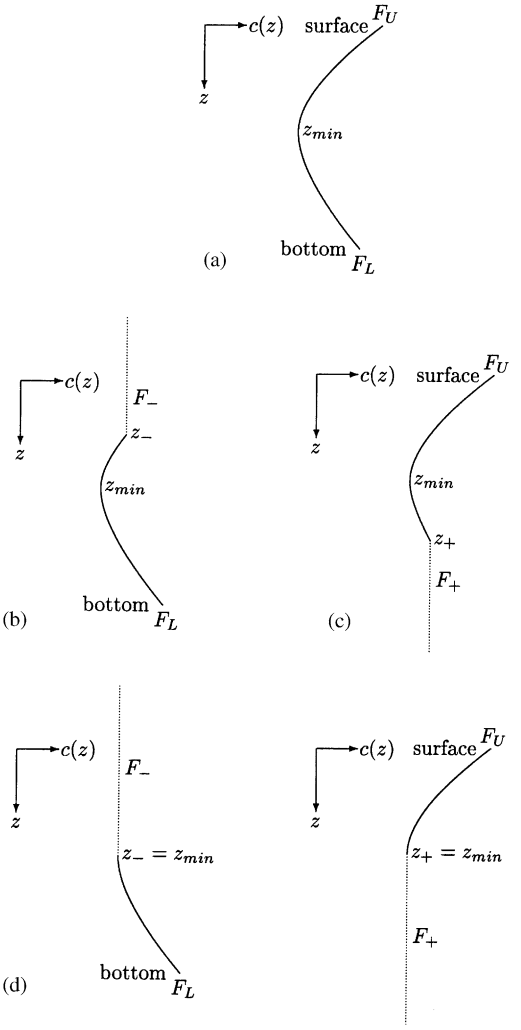

Fig. 2. Sound-speed profile for an original medium (a) and some modified ones (b–d) relevant to an understanding of possible trapped-mode contamination for the travelling-wave field components. In (b–d), the modification is indicated by the dotted curve, which may be for a constant (as shown) or '$1/c^2$ linearly decreasing' (in the outward direction) sound speed in a terminating half-space. A sound channel with mode trapping appears in (b) and (c), for $z_- < z_{min}$ and $z_+ > z_{min}$, respectively. Trapped modes do not exist for the modified media in panel (d), for which both specification depths have been located at the point z_{min} of minimum sound speed.

Eqs. (8)–(11) at points p where $W(F_U, F_+)$ or $W(F_L, F_-)$ vanishes. The $W(F_L, F_-) = 0$ singularities correspond to modes for the medium modified above z_- in accordance with upper boundary conditions represented by F_-. For $z_- < z_{min}$, see Fig. 2b, it would support trapped modes with mode function $F_-(z)$, and $P_{3,0}$ would (by Eq. (10)) be contaminated at long ranges by standing-wave energy that should preferably have been distributed exclusively among higher-j components. Similarly, the $W(F_U, F_+) = 0$ singularities correspond to modes for the medium modified below z_+ in accordance with lower boundary conditions represented by F_+. For $z_+ > z_{min}$, see Fig. 2c, trapped modes would appear and $P_{2,0}$ would be contaminated.

It follows that the specification depths should be chosen such that $z_- \geqslant z_{min}$ and $z_+ \leqslant z_{min}$. Since $z_- \leqslant z_+$ is required, $z_- = z_+ = z_{min}$ follows. The corresponding modified media are shown in Fig. 2d. Having monotonous sound-speed profiles, they do not support trapped modes. □

An alternative possibility for defining F_- or F_+ would be to consider the profile as locally '$1/c^2$ linear' at z_- or z_+. $F_-(z_-)$ or $F_+(z_+)$, respectively, could then be defined by Airy functions in order to get a purely outgoing wave far out in the implied half-space. To avoid trapped-mode contamination, however, the sound speed should not increase in the outward direction.

2.3. Convergence of the slowness integrals

Choosing $z_- = z_+$, as required by Proposition 1, is unfortunately not possible (unless $z_s = z$). Remarkably, the slowness integrals in Eq. (3) would diverge at infinity.

Proposition 2. *Assuming $r > 0$, and disregarding constant sound-speed profiles, the necessary and sufficient condition for convergence at infinity of the integral defining $P_{1,0}$ becomes*

$$|z_s - z_-| + |z_+ - z| \leqslant z_+ - z_-. \tag{12}$$

Recall that z_s is the uppermost source depth and that z is below all sources.

Proof. From Eqs. (3) and (8), the integrand for $P_{1,0}(r, z)$ will be proportional to

$$W^{-1}(F_-, F_+) F_-(z_s) F_+(z) \mathrm{H}_0^{(1)}(\omega p r) p \tag{13}$$

for a single symmetric point source at depth z_s. For simplicity, constant density is assumed and F_-, F_+ are defined at z_-, z_+ by local homogeneity. It follows from the WKBJ approximation that $F_-(z_+) \approx F_+(z_-) \approx \exp(\omega p(z_+ - z_-))$ for large p. Forming the Wronskian at z_- or z_+,

$$W^{-1}(F_-, F_+) \approx -\frac{\rho}{2\omega p} \mathrm{e}^{-\omega p(z_+ - z_-)} \quad \text{and} \quad F_-(z_s) \sim \mathrm{e}^{\omega p|z_s - z_-|}, \quad F_+(z) \sim \mathrm{e}^{\omega p|z_+ - z|}. \tag{14}$$

Putting things together, for large positive p, the essential integrand factor will appear as

$$-\frac{\rho}{2\omega} \mathrm{e}^{-\omega p[(z_+ - z_-) - |z_s - z_-| - |z_+ - z|]} \mathrm{H}_0^{(1)}(\omega p r), \tag{15}$$

and condition (12) follows. The extension to a vertical source array is straightforward. □

Assuming Eq. (12), it appears from computational tests that γ_A and γ_B are small enough to make the remaining $P_{i,j}$ well-defined and series (3) convergent. Although it remains to give a stringent proof, theoretical arguments can also be given to make this plausible. In the propagating regime, the reflection-coefficient character of γ_A and γ_B will make their product small. For large p and 'local homogeneity' specification, smallness estimates are derivable from the WKBJ approximation in the evanescent regime.

It may be inappropriate to choose specification depths that do not enclose the source and receiver depths, even if Eq. (12) is fullfilled. If the sound speed increases above z_-, a high-frequency $F_-(z_s)$ will suddenly become very large for z_s above z_- when p is increased through $1/c(z_-)$. As p is increased further, the growth of $F_-(z_s)$ will indeed be counteracted by the decrease of $W^{-1}(F_-, F_+)$ according to Eq. (14). However, $W^{-1}(F_-, F_+)$ need not be very small for p close to $1/c(z_-)$ if the maximum sound speed between z_- and z_+ is at z_-, and $P_{1,0}(r, z)$ could become anomalously large. If the sound speed increases below z_+, anomalies may likewise appear for z below z_+.

3. Recombinant travelling-wave field decompositions

The clue to resolving the conflicting requirements of Propositions 1 and 2 is to combine terms of different i types from Eqs. (8)–(11). The notation $G_{12,j} = G_{1,j} + G_{2,j}$, etc., is introduced and restriction is still made to z below all sources. Three different recombinant decompositions will be considered. Concerning $G_{12,j}$ and $G_{34,j}$ it follows, since $F_- + \gamma_A F_+$ is proportional to F_U,

$$G_{12,j}(z) = W^{-1}(F_U, F_+)W(F_U, \Phi)\gamma_A^j \gamma_B^j F_+(z), \tag{16}$$

$$G_{34,j}(z) = W^{-1}(F_U, F_+)W(F_U, \Phi)\gamma_A^j \gamma_B^{j+1} F_-(z). \tag{17}$$

Concerning $G_{13,j}$ and $G_{24,j}$, it follows that

$$G_{13,j}(z) = W^{-1}(F_-, F_L)W(F_-, \Phi)\gamma_A^j \gamma_B^j F_L(z), \tag{18}$$

$$G_{24,j}(z) = W^{-1}(F_-, F_L)W(F_+, \Phi)\gamma_A^{j+1} \gamma_B^j F_L(z). \tag{19}$$

Concerning $G_{1234,j} = G_{1,j} + G_{2,j} + G_{3,j} + G_{4,j}$, finally,

$$G_{1234,j}(z) = W(F_-, F_+)W^{-1}(F_U, F_+)W(F_U, \Phi)\gamma_A^j \gamma_B^j W^{-1}(F_-, F_L)F_L(z). \tag{20}$$

For the recombinant-type integrals, the notation $P_{12,j} = P_{1,j} + P_{2,j}$, etc., is used. An important point is that, under the conditions stated below, these quantities can be computed directly, even when the terms of the original decomposition (3) are divergent or are anomalously large such that loss of numerical precision by cancellation would result at an explicit addition.

Proposition 3. *The condition for convergence at infinity of the slowness integrals is relaxed to*

$$|z_+ - z| \leqslant z_+ - z_s \tag{21}$$

for the $P_{12,j}$, $P_{34,j}$ *decomposition* (16)–(17), *and to*

$$|z_s - z_-| \leqslant z - z_- \tag{22}$$

for the $P_{13,j}, P_{24,j}$ decomposition (18)–(19). *The slowness integrals for the $P_{1234,j}$ decomposition* (20) *converge at infinity for any choice of specification depths* (*such that $z_- \leqslant z_+$*).

Proof. The proof of Proposition 2 is readily adapted by noting that

$$F_U(z) \sim e^{\omega p z} \quad \text{and} \quad F_L(z) \sim e^{\omega p (z_b - z)} \tag{23}$$

for *all* z between the surface at depth 0 and the bottom at depth z_b. □

Corollary 4. *Now locate both specification depths at the point z_{min} of minimum sound speed in accordance with Proposition* 1.

(i) *The $P_{12,j}, P_{34,j}$ decomposition is useful at least when z, and then also z_s, are above z_{min}.*
(ii) *The $P_{13,j}, P_{24,j}$ decomposition is useful at least when z_s, and then also z, are below z_{min}.*
(iii) *The $P_{1234,j}$ decomposition is always well defined.*

Proof. Proposition 3 is applied with the observation in mind that was made in the last paragraph of Section 2.3. The implication is that z_s should preferably not be above z_- in connection with Eq. (18) if the sound speed increases upwards through z_-, and that z should preferably not be below z_+ in connection with Eq. (16) if the sound speed increases downwards through z_+. □

3.1. Examples

The '$1/c^2$ linear' downward refracting profile from Fig. 1 is chosen, with sound speed decreasing from 1.500 km/s at the pressure-release surface ($z = 0$ m) to 1.480 km/s at the flat bottom ($z = 80$ m). Below $z = 80$ m, there is a homogeneous fluid half-space with density 2 kg/dm^3, velocity 1.5 km/s, and absorption 0.66 dB/wavelength. The source and receiver depths are 10 and 80 m, respectively, and the frequency is 3 kHz. With the recombinant $P_{12,j}, P_{34,j}$ decomposition (16)–(17), z_- and z_+ can now both be located at the bottom, as prescribed by Proposition 1. A propagator-matrix scheme [18] is used for numerical computations.

The results are nicely behaved, see Fig. 3. Each field component decreases steadily beyond its caustic, cf., Fig. 1, at least down to levels of about −200 dB, where numerical noise appears. Thus, the cycle 0 ($j = 0$) components drop off sharply beyond the boundary-produced caustic at 1.3 km, the cycle 1 ($j = 1$) components beyond 3.25 km (1.3 km plus one cycle distance 1.95 km), the cycle 2 ($j = 2$) components beyond 5.2 km, etc. The only clear difference between the $P_{12,j}$ and $P_{34,j}$ fields is a reduction of amplitude for the latter caused by reflection loss at the bottom. The oscillations well ahead of the caustics in Fig. 3 are caused by interference among up- and down-going waves that is not resolved when i types have been combined. However, the original decomposition (3) with appropriately chosen specification depths works at these close ranges.

An example with a sound channel, see Fig. 4a, is also considered. The subbottom (homogeneous half-space) and frequency (3 kHz) of the previous example are retained. Source and receiver depths are first taken at 10 and 70 m, respectively. The total-field transmission loss as a function of range will get a peak structure caused by refraction back and forth in the sound channel and, see Fig. 4b, the recombinant $P_{1234,j}$ decomposition (20) successfully distributes

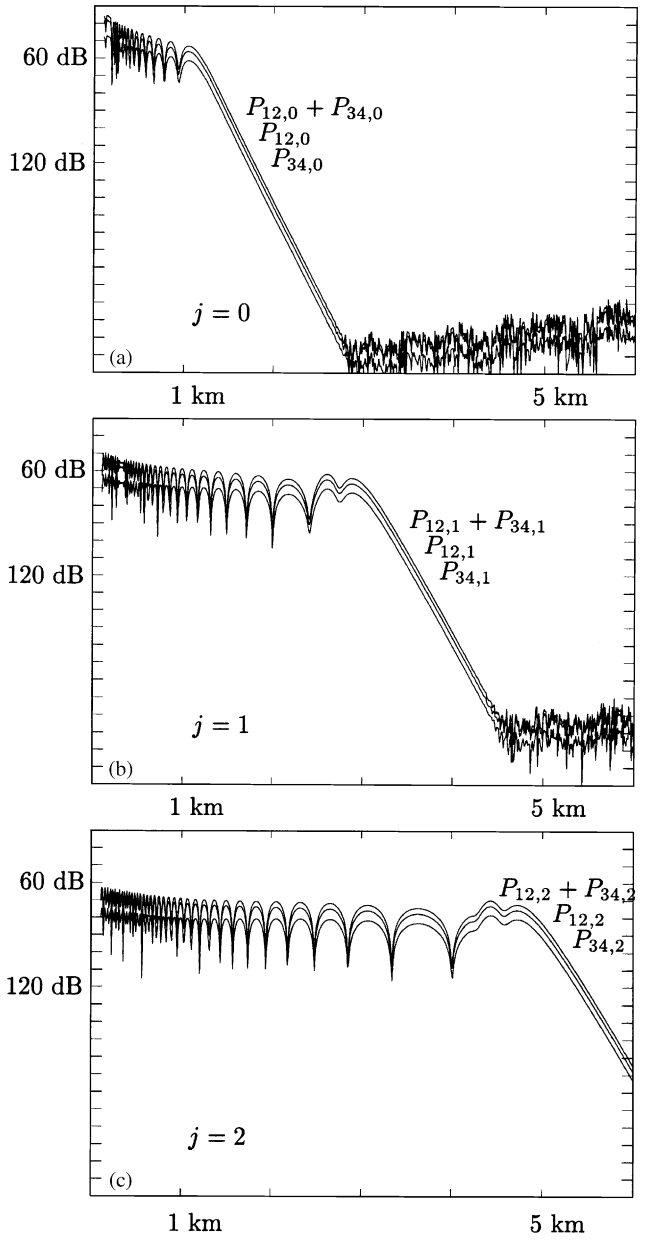

Fig. 3. Transmission loss (re 1 m) for the recombinant-decomposition components $P_{12,j}$ and $P_{34,j}$ for the downward refracting medium with $z_- = 80$ m (local homogeneity) and $z_+ = 80$ m (local '$1/c^2$ linearity'). (a), (b) and (c) concern the cycle numbers $j = 0$, 1 and 2, respectively. The coherent sum $P_{1234,j}$ of the $P_{12,j}$ and $P_{34,j}$ field components is also shown in each case.

physical ray energy into terms with appropriate cycle numbers. In accordance with Proposition 1, both specification depths z_- and z_+ have been placed at the depth of minimum sound speed (40 m). This choice is critical. With the receiver depth raised to 20 m, the recombinant $P_{12,j}, P_{34,j}$

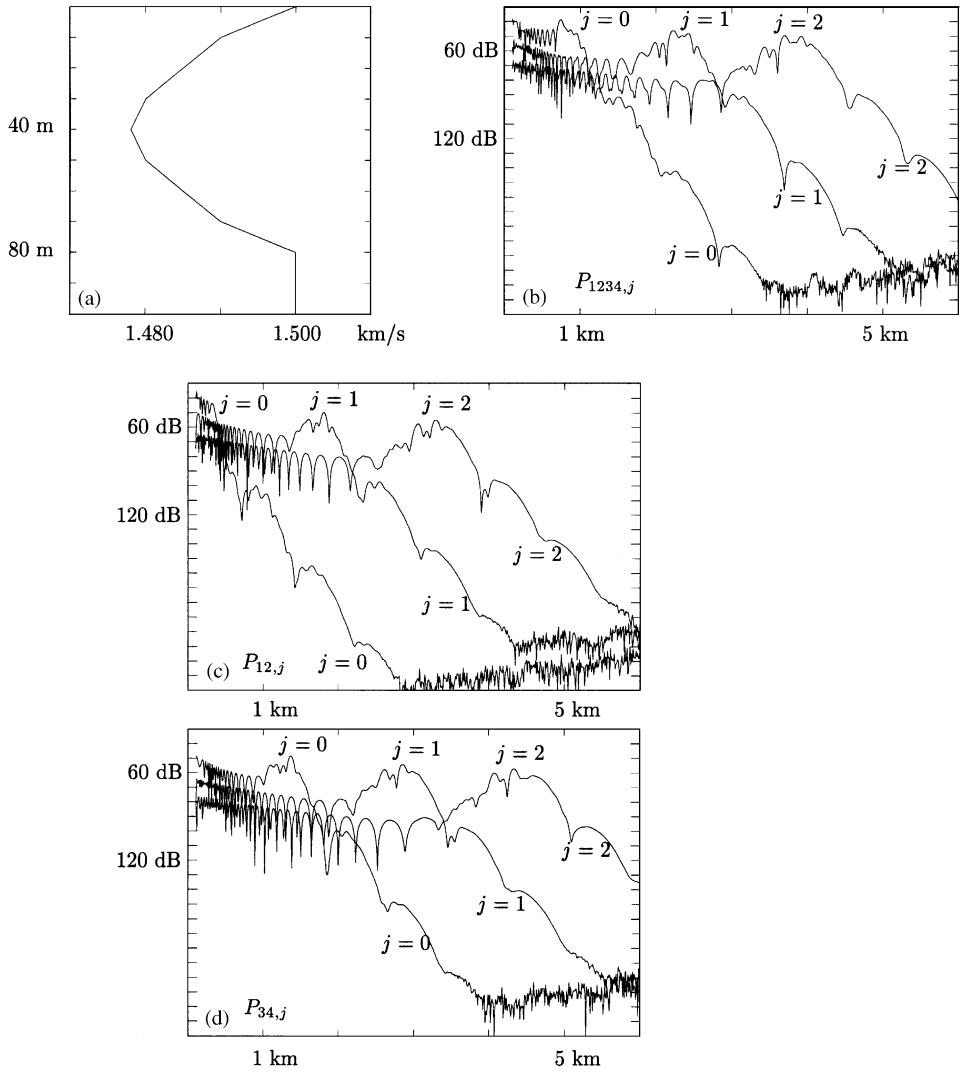

Fig. 4. An example with a sound channel. Transmission loss (re 1 m) is shown for recombinant-decomposition components with 'local homogeneity' specification of F_-, F_+ at $z_- = z_+ = 40$ m. (a) The sound-speed profile. (b) $P_{1234,j}$ according to Eq. (20) for source and receiver depths at 10 and 70 m, respectively. (c and d) $P_{12,j}$ according to Eq. (16) and $P_{34,j}$ according to Eq. (17), respectively, when the receiver depth has been changed to 20 m.

decomposition (16)–(17) can be applied (Corollary 4). The nicely behaved results are shown in Fig. 4c and d. The peaks are displaced in range in the way expected by classical ray theory.

3.2. *Leaky-mode representations of grazing-ray diffraction*

By accounting for residue contributions from poles (modes) and avoiding to cross branch cuts, the slowness integration path along the real axis for $P_{12,j}$, etc., cf., Eq. (3), can be shifted into the upper half-plane. Ignoring the typically small branch-cut integral contributions, a discrete set of

mode contributions remains for each recombinant-type field component. The corresponding residues series may diverge at close ranges, but the representation is valid close to and beyond the shadow boundary. Assuming that z_- and z_+ are both located at the point of minimum sound speed, trapped modes are avoided (Proposition 1) and all modes are *leaky*. By Eqs. (16)–(20), they arise from zeros of $W(F_U, F_+)$ and/or $W(F_L, F_-)$, cf., Fig. 2d. Components with cycle number $j \geqslant 1$ typically have higher order poles caused by the additional singularities from γ_A and γ_B, see Eq. (6).

For the example in Fig. 3, without $W(F_L, F_-) = 0$ modes, $W(F_U, F_+) = 0$ modes arise from the zeros on the negative axis for the Airy function. An infinite sequence of leaky-mode slownesses appears in the first quadrant, starting close to the surface slowness $1/1.500$ s/km and moving out to infinity in the direction $\arg(p) = \pi/6$ asymptotically. It appears [19] that some 10 leaky modes suffice for representing each $P_{12,j}$, etc., in Fig. 3 close to and beyond its shadow boundary.

Leaky modes are thus appropriate for a travelling-wave representation of these shadow-zone fields. The strictly positive imaginary part for the modal slowness p causes an exponential decrease with range r of the pertinent Hankel-function factor, suggesting a creeping-wave interpretation with ray-shedding loss. The shadow boundary appears in depth where this decrease with range is balanced by the exponential growth or decay of the leaky-mode amplitude.

For the sound channel example in Fig. 4, the crucial $W(F_U, F_+) = 0$ mode slownesses will again appear close to the grazing-ray slowness $1/1.500$ s/km in the first quadrant. Again, for each recombinant-decomposition field component, some 10 leaky modes suffice for shadow-zone representation and for a good tie to the closer region, where the original expansion (3) is adequate. In this case, there are $W(F_L, F_-) = 0$ modes as well. However, they are not related to the grazing-ray diffraction from the surface and they are not relevant for the $P_{12,0}$ component.

4. Conclusions

The terms of the traditional travelling-wave expansion of the pressure field in a laterally homogeneous acoustic medium are not well defined, since the corresponding slowness integrals are typically divergent at infinity. Convergent integrals appear by allowing different specification depths for up- and down-going waves, such that the source and receiver depths are enclosed. The resulting travelling-wave expansion is useful at close ranges for isolating generalized-ray components. It fails, however, for weak shadow-zone fields that cannot be represented by stationary-phase (or related) contributions, because of trapped-mode contamination at the longer ranges.

By combining the terms, recombinant expansions have been derived that allow useful travelling-wave representation of the problematic shadow-zone fields, exactly as well as approximately by a limited number of leaky modes. Up- and down-going waves can now be specified at the depth of minimum sound speed, and trapped-mode contributions are avoided. The shadow boundary appears where the leaky-mode amplitude is balanced by the exponential decrease with range of the Hankel-function factor. At close ranges, the leaky-mode series for each recombinant-type field component may diverge, but it can be tied to the corresponding generalized-ray components there.

Apart from its intrinsic interest, a travelling-wave field representation by a limited number of generalized-ray and leaky-mode terms is useful in connection with computation of scattered fields.

Semi-empirical scattering rules as well as more rigorous computations can be applied term-wise. A nice by-product of the presented analysis is a generalization of results for single grazing-ray diffraction, as described in Refs. [1, Chapter IX; 2, Section 9-5], to multiple grazing-ray diffraction for general sound-speed profiles.

References

[1] L.M. Brekhovskikh, Waves in Layered Media, 2nd Edition, Academic Press, New York, 1980.
[2] A.D. Pierce, Acoustics, AIP Press, New York, 1994.
[3] B.D. Seckler, J.B. Keller, Application of ray theory to acoustic propagation in horizontally stratified oceans, Journal of the Acoustical Society of America 31 (1959) 192–205.
[4] D.V. Batorsky, L.B. Felsen, Ray-optical calculation of modes excited by sources and scatterers in a weakly inhomogeneous duct, Radio Science 6 (1971) 911–923.
[5] G.A. Leibiger, Application of normal mode theory to propagation of 3.5 kHz pulses in shallow water, Vitro Laboratories Technical Memorandum VL-2476-9-0, 1968.
[6] H. Weinberg, Application of ray theory to acoustic propagation in horizontally stratified oceans, Journal of the Acoustical Society of America 58 (1975) 97–109.
[7] T.K. Kapoor, L.B. Felsen, Hybrid ray-mode analysis of acoustic scattering from a finite, fluid-loaded plate, Wave Motion 22 (1995) 109–131.
[8] P.C. Etter, Underwater Acoustic Modeling, E & FN Spoon, London, 1996.
[9] J.L. Bishop, S. Ivansson, Multipath field representation for seabed parameter extraction using backscatter data from shadow zones, in: N.G. Pace, E. Pouliquen, O. Bergem, A.P. Lyons (Eds.), High Frequency Acoustics in Shallow Water, La Spezia: SACLANTCEN Conference Proceedings CP-45, 1997, pp. 39–47.
[10] S.J. Franke, R. Raspet, C.H. Liu, Numerical predictions of atmospheric sound-pressure levels in shadow zones, Journal of the Acoustical Society of America 83 (1988) 816–820.
[11] T. Ishihara, K. Ohshima, Asymptotic analysis of acoustic field by geometrical theory of diffraction in antiwaveguide propagation, Japanese Journal of Applied Physics 32 (1993) 2483–2486.
[12] F. Jensen, W. Kuperman, M. Porter H. Schmidt, Computational Ocean Acoustics, AIP Press, New York, 1994.
[13] B.L.N. Kennett, Seismic Wave Propagation in Stratified Media, Cambridge University Press, Cambridge, 1983.
[14] E.K. Westwood, C.T. Tindle, N.R. Chapman, A normal mode model for acousto-elastic ocean environments, Journal of the Acoustical Society of America 100 (1996) 3631–3645.
[15] D.A. DiNapoli, R.L. Deavenport, Numerical models of underwater acoustic propagation, in: J.A. DeSanto (Ed.), Topics in Current Physics 8: Ocean Acoustics, Springer, Berlin, 1979, pp. 79–157.
[16] F.W. Sluijter, Arbitrariness of dividing the total field in an optically inhomogeneous medium into direct and reversed waves, Journal of the Optical Society of America 60 (1970) 8–10.
[17] T. Ishihara, L.B. Felsen, Hybrid ray-mode parametrization of high frequency propagation in an open waveguide with inhomogeneous transverse refractive index: formulation and application to a bilinear surface duct, IEEE Transactions on Antennas and Propagation 39 (1991) 780–788.
[18] S. Ivansson, The compound matrix method for multi-point boundary-value problems, Zeitschrift für angewandte Mathematik und Mechanik 77 (1997) 767–776.
[19] S. Ivansson, J. Bishop, Single and multiple grazing-ray diffraction as derived by Green's function expansion, in: M.E. Zakharia (Ed.), Proceedings of the Fifth European Conference on Underwater Acoustics ECUA 2000, European Commission, Brussels, 2000, pp. 21–26.